The 2015 World Congress on
Advances in Structural Engineering and Mechanics (ASEM15)
Incheon, Korea, August 25-29, 2015

An Efficient Method for Galloping Profile Monitoring of Power Transmission Lines by Use of an Inertial Unit: Theoretical and Experimental Investigation

Zhong-Bin Lv[1)], Qing Li[2)], *Yi-Qing Ni[3)], Qin Huang[4)], Wang-Lin Wu[5)], and Chao Zhang[6)]

[1), 2)] *State Grid Henan Electric Power Research Institute, Zhengzhou, Henan 450052, China*
[3), 5)] *Department of Civil and Environmental Engineering, The Hong Kong Polytechnic University, Hung Hom, Kowloon, Hong Kong*
[3), 5), 6)] *Research Center for Advanced Sensing and Monitoring Technology (RCASMT), PolyU Shenzhen Research Institute, Shenzhen, Guangdong 518057, China*
[4)] *Honesty Technology & Consultancy Limited, Shenzhen, Guangdong 518000, China*
[3)] ceyqni@polyu.edu.hk

ABSTRACT

In the last few decades, a great deal of research has been devoted to tracking the galloping profile of power transmission lines. However, the conventional methods couldn't account for the torsion effect of cross section of the transmission lines. This paper presents a new method for capturing the galloping track of transmission lines based on an inertial measurement unit (IMU), in which both linear accelerations and angular velocities of the transmission line are measured. The attitude of IMU is calculated by a quaternion algorithm and updated with the aid of a gradient descent fusion algorithm. With the obtained attitude of IMU, the three measured linear accelerations are rectified by coordinate transformation, and the gravitational acceleration is filtered from the rectified accelerations. Then the three-dimensional galloping track of the transmission line is captured through integration of the corrected acceleration data in the time domain. The feasibility of the proposed method is demonstrated through laboratory experiments using a galloping testing machine situated in the State Grid Key Laboratory of Power Overhead Transmission Line Galloping (Zhengzhou, China), where different types of motion are executed. The experimental results show that by taking into account the torsion effect of cross section of the transmission line, the proposed method can accurately identify the vibration characteristics (amplitude and frequency) of the transmission line during galloping and satisfactorily reconstruct the galloping track of the transmission line in real time.

Keywords: Power transmission line; Galloping; Profile monitoring; Torsion effect; Inertial measurement unit (IMU).

1. INTRODUCTION

Galloping of iced power transmission lines with non-circular cross sections is in general characterized by low frequency (0.1~3.0 Hz), large amplitude (above 10 m at maximum) (Desai et al. 1996; Huang et al. 2011), and self-excited oscillation due to aerodynamic forces (Desai et al. 1995). Galloping under certain flow and climate conditions may bring about excessive vibrations of iced transmission lines and damage of conductors and tower components (Desai et al. 1996).

The phenomena of galloping, first documented as early in 1932 (Den Hartog 1932), has been extensively investigated in the past decades. In addition to analytical studies (Den Hartog 1932; Nigol and Clarke 1974; Desai et al. 1990; Yu et al. 1993a, b) and numerical simulations (Desai et al. 1995; Liu et al. 2009), experiments and field observations were also made to support the study of transmission line galloping. The galloping profile tracking is one of the most important issues on the monitoring of power transmission lines. A number of methods have been proposed for tracking galloping profile, mainly including image target tracking-based methods and linear accelerometer-based methods (Liu et al. 2014). The image target tracking-based methods monitor the galloping profile of transmission lines by image processing techniques that analyze galloping videos frame-by-frame. The accuracy of these methods is susceptible to the weather condition and the distance between the camera and the target.

The linear accelerometer-based methods obtain transmission line galloping profile through processing of the measured accelerations. Using acceleration sensors and wireless units, Huang et al. (2009, 2011) proposed an online galloping profile monitoring method for transmission lines, and proved via simulations that it performed well in anti-noise and real-time. To improve the measurement accuracy, Rui et al. (2011) proposed another online galloping monitoring method for transmission lines based on two degree-of-freedom fiber grating acceleration sensors. However, these linear accelerometer-based methods couldn't take into consideration the torsion effect of cross section of the transmission lines.

The torsion effect cannot be ignored because it may result in significant errors in galloping amplitude identification even if the galloping frequency is correctly identified (Wang et al. 2010). When galloping occurs, the motion of transmission lines is actually a combination of translation and rotation, and gravitational acceleration will bring about components in the test-point-fixed coordinate directions. Therefore, the measurement values obtained by linear accelerometers fixed on the transmission lines are the sum of motion accelerations and gravitational acceleration components rather than the motion accelerations themselves. To filter out the gravitational acceleration components from the measured accelerations, it is necessary to obtain the orientation relationship between the test-point-fixed coordinate system and the geographic coordinate systems through measuring angular acceleration or angular velocity of the transmission line when galloping occurs.

This paper presents a new method for capturing the galloping track of transmission lines based on inertial measurement unit (IMU), in which both linear accelerations and angular velocities of the transmission line are measured. Making use

of three translations and three rotations, the attitude of IMU is updated in real time through a gradient descent fusion algorithm, and the three measured linear accelerations are rectified by coordinate transformation accordingly. By the gravitational acceleration filtering, the gravitational acceleration components are filtered from the rectified acceleration. Then the three-dimensional galloping track of the transmission line is captured by eliminating the gravitational acceleration components in the time domain. The feasibility of the proposed method is experimentally demonstrated by imposing different types of motion with a galloping testing machine situated in the State Grid Key Laboratory of Power Overhead Transmission Line Galloping, Zhengzhou, China.

2. THEORETICAL DEVELOPMENT

To account for the torsion effect of cross section of transmission lines, the attitude of IMU is first determined by a quaternion algorithm and updated with the aid of a gradient descent fusion algorithm. With the updated attitude of IMU, the measured accelerations are rectified by coordinate transformation, and the gravitational accelerations are filtered from the rectified accelerations. By integration of the corrected acceleration data in the time domain, galloping track of the transmission line is captured.

2.1 ATTITUDE CALCULATION BY QUATERNION ALGORITHM

The linear accelerations are measured in terms of the IMU-fixed coordinate system. To transform the measurements from the IMU-fixed coordinate system to the geographic coordinate system, the attitude of IMU needs to be determined. In order to reduce accumulative error in the integration process of angular velocities, which are measured by IMU, a quaternion algorithm is adopted to determine the attitude of IMU.

The attitude of IMU at time step *t* can be expressed in the quaternion form as

$$ {}^{S}_{E}\mathbf{q}_t = q_{0,t} + q_{1,t}\boldsymbol{i} + q_{2,t}\boldsymbol{j} + q_{3,t}\boldsymbol{k} \tag{1} $$

where $q_{1,t}$, $q_{2,t}$, $q_{3,t}$ are real quantities and $\boldsymbol{i}$, $\boldsymbol{j}$, $\boldsymbol{k}$ are imaginary units. The quaternion form in Eq. (1) could be understood as a spatial rotation, where the rotation axis is determined by the combination of $q_{1,t}\boldsymbol{i}$, $q_{2,t}\boldsymbol{j}$ and $q_{3,t}\boldsymbol{k}$ and the rotation angle is calculated by $q_{0,t}$. The superscript *S* denotes the IMU-fixed coordinate system while the subscript *E* represents the geographic coordinate system.

The attitude quaternion ${}^{S}_{E}\mathbf{q}$ at time step *t*+1 can be obtained by using the first order Runge-Kutta method as

$$ {}^{S}_{E}\mathbf{q}_{t+1} = {}^{S}_{E}\mathbf{q}_t + {}^{S}_{E}\dot{\mathbf{q}}_t \Delta t \tag{2} $$

where ${}^{S}_{E}\mathbf{q}_t$ is the value of attitude quaternion ${}^{S}_{E}\mathbf{q}$ at time step *t*, ${}^{S}_{E}\dot{\mathbf{q}}_t$ is the derivative of ${}^{S}_{E}\mathbf{q}_t$, and Δt represents the sampling interval. The derivative of attitude quaternion at each time step is obtained from the angular velocity measured at the present time step and the attitude quaternion at the previous time step. That is

$$ {}^{S}_{E}\dot{\mathbf{q}}_t = \frac{1}{2} {}^{S}_{E}\mathbf{q}_{t-1} \otimes {}^{S}\boldsymbol{\omega}_t \tag{3} $$

in which ${}^{S}\boldsymbol{\omega}_t$ is the angular velocity collected from IMU at time step *t* in IMU-fixed coordinate system, ${}^{S}_{E}\mathbf{q}_{t-1}$ represents the value of attitude quaternion ${}^{S}_{E}\mathbf{q}$ at time step *t*-1, and the symbol $\otimes$ denotes the Kronecker product.

2.2 ATTITUDE UPDATING BY GRADIENT DESCENT FUSION ALGORITHM

The attitude quaternion ${}^{S}_{E}\mathbf{q}$ at time step *t*+1 can be calculated by Eq. (2) directly. However, the accumulative errors might result in large drift as time goes on. To reduce the accumulative errors, the attitude quaternion of IMU is updated at each time step by a gradient descent fusion algorithm (Madgwick et al. 2011).

Because the linear accelerations measured by IMU are usually much smaller than the gravitational acceleration, so the error function can be defined as

$$ \mathbf{f}_t = {}^{S}\mathbf{g}_t - {}^{S}\mathbf{a}_t \tag{4} $$

where ${}^{S}\mathbf{g}_t$ is the gravitational acceleration in the IMU-fixed coordinate system at time step *t*, and ${}^{S}\mathbf{a}_t$ is the linear acceleration measured by IMU in the IMU-fixed coordinate system at time step *t*.

The gravitational acceleration is constant in the geographic coordinate system, denoted as ${}^{S}\mathbf{g}_t = [0\ 0\ -1]$. By introducing a coordinate transformation matrix, the gravitational acceleration can be transformed from the geographic coordinate system to the IMU-fixed coordinate system as

$$ {}^{S}\mathbf{g}_t = \left[{}^{E}_{S}\mathbf{C}_t \right]^{-1} {}^{E}\mathbf{g}_t \tag{5} $$

in which,

$$ {}^{E}_{S}\boldsymbol{C}_t = \begin{bmatrix} (q_{0,t}^2 + q_{1,t}^2 - q_{2,t}^2 - q_{3,t}^2) & 2(q_{1,t}q_{2,t} - q_{0,t}q_{3,t}) & 2(q_{1,t}q_{3,t} + q_{0,t}q_{2,t}) \\ 2(q_{1,t}q_{2,t} + q_{0,t}q_{3,t}) & (q_{0,t}^2 - q_{1,t}^2 + q_{2,t}^2 - q_{3,t}^2) & 2(q_{2,t}q_{3,t} - q_{0,t}q_{1,t}) \\ 2(q_{1,t}q_{3,t} - q_{0,t}q_{2,t}) & 2(q_{2,t}q_{3,t} + q_{0,t}q_{1,t}) & (q_{0,t}^2 - q_{1,t}^2 - q_{2,t}^2 + q_{3,t}^2) \end{bmatrix} \tag{6} $$

where ${}^{S}_{E}\boldsymbol{C}_t$ is the coordinate transformation matrix that makes transformation from the IMU-based coordinate system to the geographic coordinate system at time step *t*, and the values of $q_{0,t}$, $q_{1,t}$, $q_{2,t}$, $q_{3,t}$ are taken from the updated attitude quaternion ${}^{S}_{E}\mathbf{q}_{upd,t-1}$ at time step *t*-1.

The gradient of the error function can be calculated as

$$\nabla \mathbf{f}_t = \mathbf{J}_t' \mathbf{f}_t \tag{7}$$

where $\nabla \mathbf{f}_t$ represents the gradient of the error function, and $\mathbf{J}_t$ denotes the Jacobian matrix of the error function.

Then the attitude quaternion at time step *t* can be updated from Eq. (2) as follows (Madgwick et al. 2011)

$$\overset{S}{E}\mathbf{q}_{upd,t} = \overset{S}{E}\mathbf{q}_{upd,t-1} + \overset{S}{E}\dot{\mathbf{q}}_{upd,t}\Delta t \tag{8}$$

where

$$\overset{S}{E}\dot{\mathbf{q}}_{upd,t} = \overset{S}{E}\dot{\mathbf{q}}_t - \beta \frac{\nabla \mathbf{f}_t}{\left\| \nabla \mathbf{f}_t \right\|} \tag{9}$$

in which $\overset{S}{E}\mathbf{q}_{upd,t}$ and $\overset{S}{E}\mathbf{q}_{upd,t-1}$ are the updated attitude quaternions at time steps *t* and *t*-1, respectively. $\overset{S}{E}\dot{\mathbf{q}}_t$ is the derivative of attitude quaternion calculated by Eq. (3), and β is the convergence factor of the gradient descent fusion algorithm.

2.3 ACCELERATIONS RECTIFIED AND GRAVITATIONAL ACCELERATION FILTERING

Since the attitude of IMU at time step *t* is calculated as $\overset{S}{E}\mathbf{q}_{upd,t}$, the coordinate transformation matrix $\overset{S}{E}\boldsymbol{C}_t$ can be modified by Eq. (6), in which the values of $q_{0,t}$, $q_{1,t}$, $q_{2,t}$, $q_{3,t}$ are taken from the updated attitude quaternion $\overset{S}{E}\mathbf{q}_{upd,t}$ at time step *t*. Accordingly, the linear accelerations $^{S}\mathbf{a}_t$ measured by IMU in the IMU-fixed coordinate system can be transformed to the geographic coordinate system as

$$^{E}\mathbf{a}_t = \overset{E}{S}\mathbf{C}_t \, ^{S}\mathbf{a}_t \tag{10}$$

where $^{S}\mathbf{a}_t$ is the linear acceleration in the geographic coordinate system. Then the gravitational acceleration can be filtered from the measured linear accelerations as

$$^{E}\mathbf{a}_{motion,t} = ^{E}\mathbf{a}_t - ^{E}\mathbf{g}_t \tag{11}$$

where $^{E}\mathbf{a}_{motion,t}$ is the motion acceleration of IMU at time step *t*.

2.4 GALLOPING TRACK RECONSTRUCTION

The linear motion velocity of IMU at time step *t* is obtained by integration of the linear motion acceleration $^{E}\mathbf{a}_{motion,t}$ in the time domain as

$$^{E}\mathbf{v}_t = {}^{E}\mathbf{v}_{t-1} + {}^{E}\mathbf{a}_{motion,t}\Delta t \tag{12}$$

where $^{E}\mathbf{v}_t$ and $^{E}\mathbf{v}_{t-1}$ are the linear motion velocities of IMU at time steps *t* and *t*-1, respectively.

Then, by integrating the linear motion velocity $^{E}\mathbf{v}_{t-1}$, the linear motion displacement of IMU at time step *t* can be calculated as

$$^{E}\mathbf{s}_t = {}^{E}\mathbf{s}_{t-1} + {}^{E}\mathbf{v}_t\Delta t \tag{13}$$

where $^{E}\mathbf{s}_t$ and $^{E}\mathbf{s}_{t-1}$ are the linear motion displacements of IMU at time steps *t* and *t*-1, respectively.

Zero-phase digital filter (Mitra and Kuo 2006) is used in the above two integrations to reduce the integral drifting. The flow chart of IMU data processing for reconstructing the galloping track of transmission lines is shown in Figure 1.

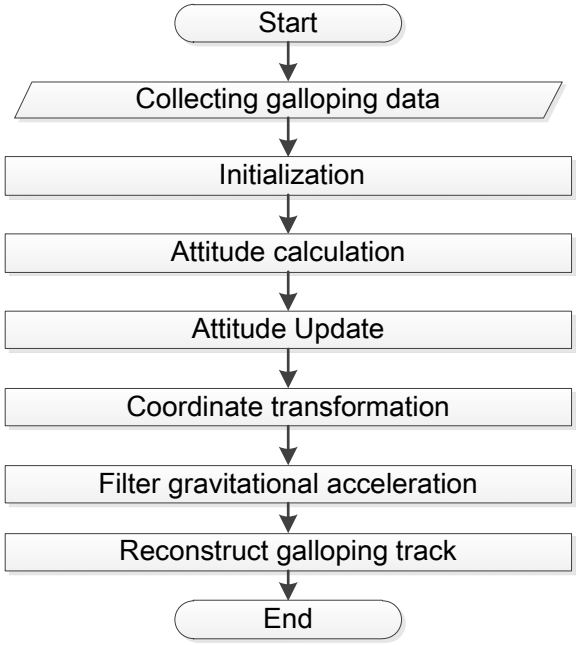

Figure 1. Flow chart of IMU data processing

3. EXPERIMENTAL INVESTIGATION

To verify the feasibility and accuracy of the proposed galloping profile monitoring method for transmission lines, a series of experiments have been conducted using a galloping testing machine situated in the State Grid Key Laboratory of Power Overhead Transmission Line Galloping, Zhengzhou, China.

3.1 TRANSMISSION LINE MODEL

Aluminum clad steel wire, which is the most widely used transmission line for transmission voltage over 10 kV in China, is chosen as the transmission line model in this study. In the aluminum clad steel wire, steel wire is used to transmit current while aluminum is used to wrap steel wire and reduce corona losses. The size of cross section of aluminum clad steel wire is dependent on the target transmission voltage. The LGJ-300/40 aluminum clad steel wire used in this study has 7 steel strands with a diameter of 2.66 mm as a core and 24 aluminum wire strands with a diameter of 3.99 mm as wrapping material. The specification of the LGJ-300/40 aluminum clad steel wire is shown in Table 1.

Table 1. Specification of LGJ-300/40 aluminium-conductor steel-reinforced (ACSR)

Nominal sectional area (aluminium / steel)		300 mm^2 / 40 mm^2
Strand number / strand diameter	aluminium	24 / 3.99 mm
	steel	7 / 2.66 mm
Outer diameter		23.94 mm
DC resistance		≤ 0.09614 Ω/km^{-1}
Weight per length		1.133 kg/m
Elastic modulus		7300 kN/mm^2

(a) Transmission line (b) Monocular vision inspection system

Figure 2. Experimental set-up

3.2 INSTRUMENTATION

Different types of vibration pattern were tested in the laboratory, and a monocular vision inspection system is also used as a reference. A galloping testing machine, as shown in Figure 2(a), is used to excite different vibration motions, including vertical vibration motion, horizontal vibration motion, and nearly circular vibration motion. For the purpose of comparison and verification, a high-resolution monocular vision

inspection system, as shown in Figure 2(b), is used to record the image signals of vibration and derive the motion profile by using an inter-frame differential method (Hu 2008). The distance between the target point and the video camera, the elevation angle, and the horizontal angle are measured by a laser rangefinder for the purpose of calibrating the image signals to motion profiles. The location to mount IMU is chosen same as the target point for monocular vision inspection.

3.3 TEST CASES AND PROCEDURES

As shown in Table 2, three cases with different vibration patterns are considered in the experiments. All these cases are tested in the following procedures:

(1) Keep the IMU in the horizontal direction and keep it static on the power transmission line for 20 seconds;

(2) Activate the galloping testing machine to work, and maintain the galloping frequency at about 1 Hz;

(3) Stop the galloping testing machine after galloping has happened for 60 seconds;

(4) Analyze the measurement data and reconstruct galloping track of the power transmission line.

Table 2. Test cases with different vibration patterns

Galloping state	Frequency	Initial static time	Motion time	Position relationship between IMU (target point) and camera		
				Linear distance	Elevation angle	Horizontal angle
Vertical motion	0.9693 Hz	20 s	60 s	5.6 m	1.6°	134.6°
Horizontal motion	0.8748 Hz	20 s	60 s	5.6 m	1.6°	134.6°
Circular motion	0.8743 Hz	20 s	60 s	5.6 m	1.6°	134.6°

3.4 EXPERIMENTAL RESULTS

The IMU is kept in the horizontal direction and in static equilibrium on the power transmission line for 20 seconds before starting each test. The galloping vibration lasts for 60 seconds in each test case. The galloping tracks of the power transmission line with vertical motion, horizontal motion, and nearly circular motion identified by IMU and monocular are shown in Figures 3 to 5, respectively. It can be seen that the proposed IMU reliably recognizes the vibration patterns, and the tracked galloping profile by IMU in each case is closely coincident with that identified by monocular. The displacement time histories of the power transmission line with vertical motion, horizontal motion, and

approximate circular motion identified by IMU and monocular are shown in Figures 6 to 8, respectively. The results show that the proposed IMU enables the reconstruction of galloping tracks of the power transmission line.

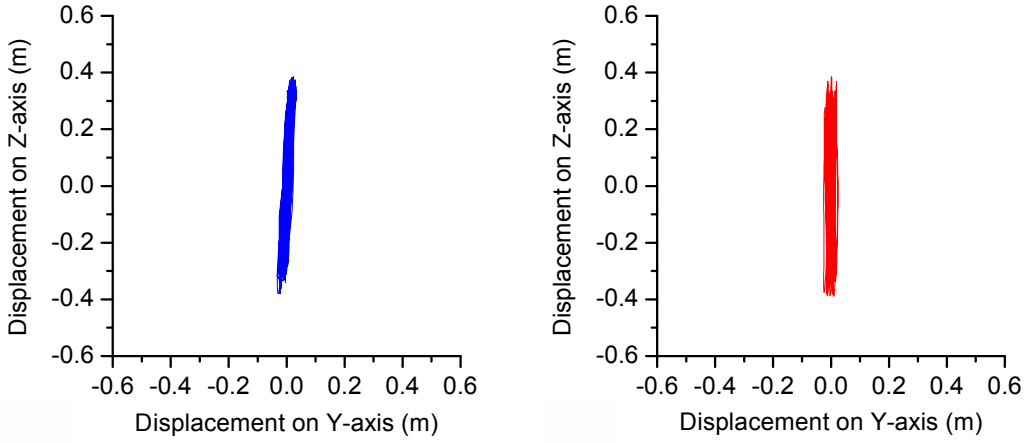

(a) Monocular (b) IMU

Figure 3 Comparison of tracked galloping profiles in vertical motion

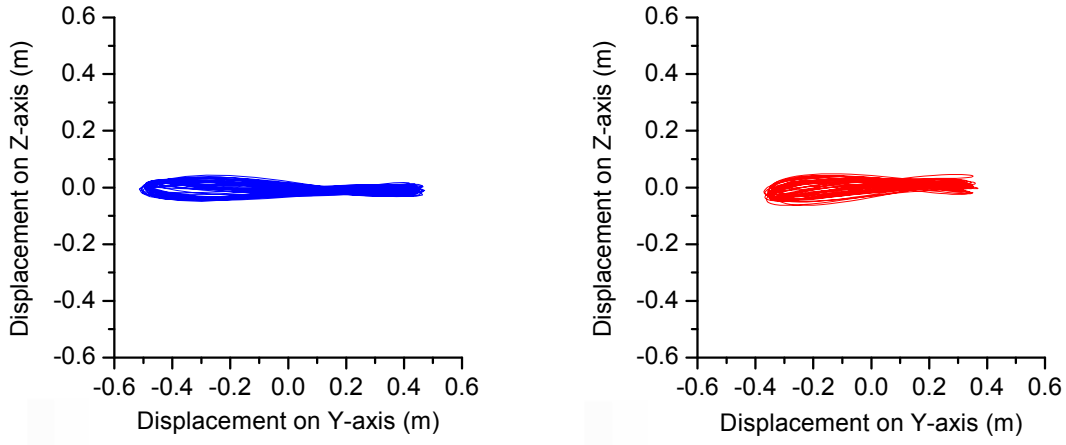

(a) Monocular (b) IMU

Figure 4 Comparison of tracked galloping profiles in horizontal motion

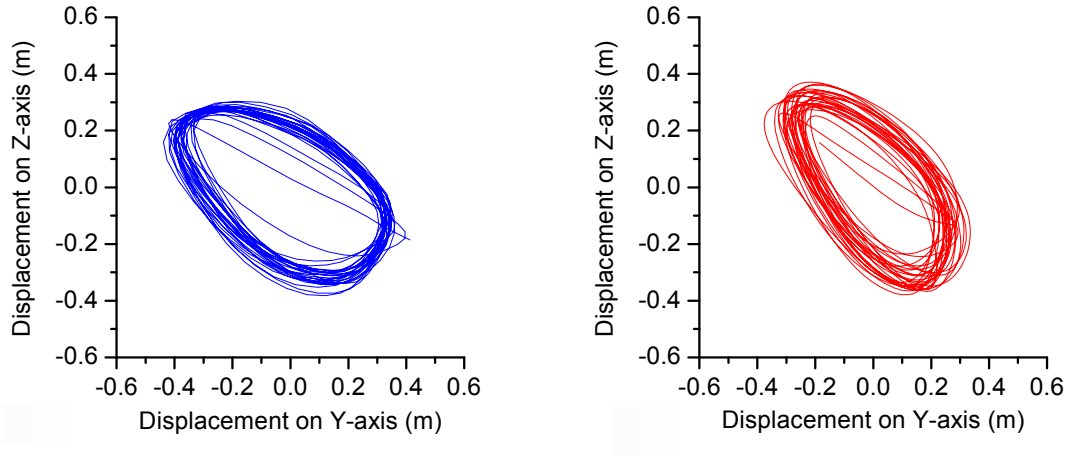

(a) Monocular (b) IMU

Figure 5 Comparison of tracked galloping profiles in nearly circular motion

The average amplitudes and galloping frequency identified by IMU and monocular are shown in Table 3. The average amplitude is defined as the average value of all the extreme points over the time history, and the difference is calculated in reference to the values identified by monocular. It is seen that the differences between the galloping frequencies identified by IMU and monocular are less than 1%. The average amplitudes in vertical direction identified by IMU and monocular are very close to each other, while the differences are much greater in horizontal direction. This is because the accuracy of IMU is isotropic while the accuracy of monocular is easily affected by the shooting angle of the positioned camera.

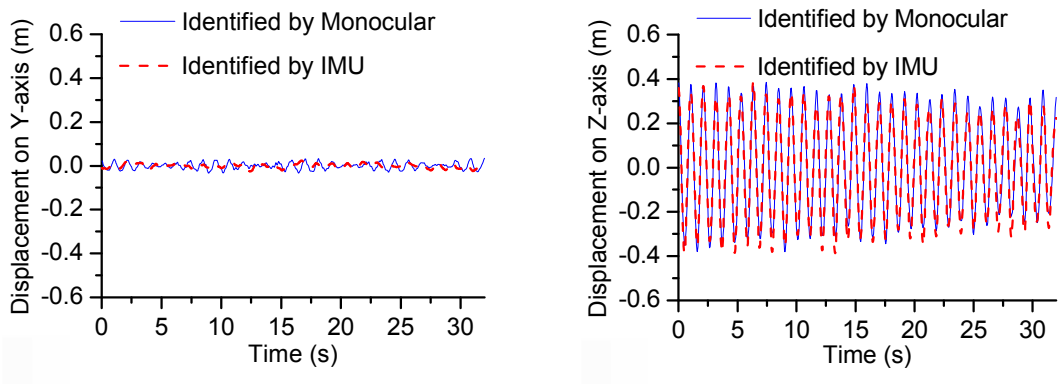

(a) Horizontal (b) Vertical

Figure 6 Comparison of displacement time histories in vertical motion

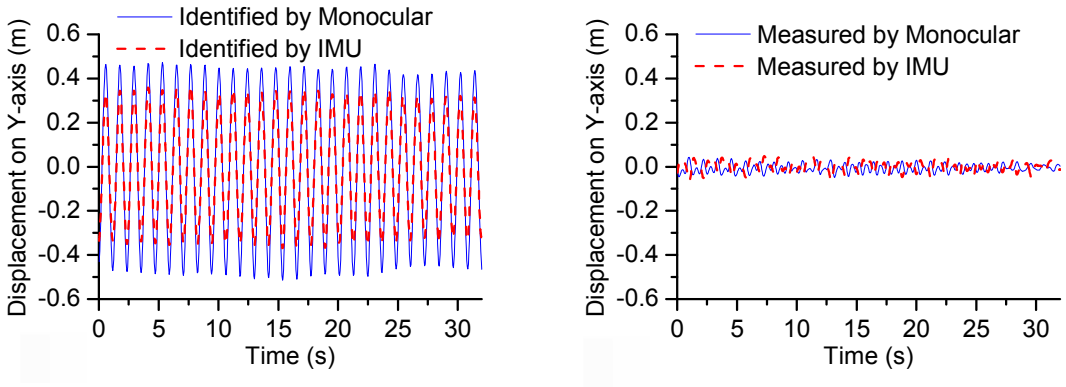

(a) Horizontal (b) Vertical

Figure 7 Comparison of displacement time histories in horizontal motion

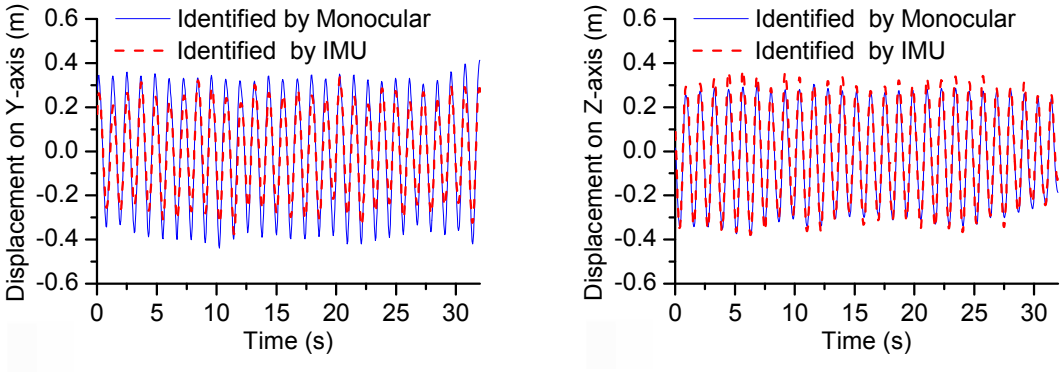

(a) Horizontal (b) Vertical

Figure 8 Comparison of displacement time histories in nearly circular motion

Table 3 Summary of experimental results

Vibration pattern	Motion direction	Mean amplitude (m)			Frequency (Hz)		
		Monocular	IMU	Difference	Monocular	IMU	Difference
Vertical motion	Y	0.0096	0.0062	35.42%	0.9693	0.9702	0.09%
	Z	0.3202	0.3069	4.15%			
Horizontal motion	Y	0.4655	0.3435	26.21%	0.8748	0.8764	0.18%
	Z	0.0204	0.0219	7.35%			
Nearly circular motion	Y	0.3635	0.2726	25.01%	0.8743	0.8743	0%
	Z	0.2948	0.3206	8.75%			

4. CONCLUSIONS

In this study, a new method for capturing the galloping track of transmission lines based on an inertial measurement unit (IMU) has been developed and experimentally verified in laboratory. To take in account the torsion effect of cross section of the transmission lines, the theoretical method to reconstruct galloping track of transmission lines from IMU monitoring data has been encoded with the following algorithms: attitude identification and updating, coordinate transformation, gravitational acceleration filtering, and quadratic integration of linear acceleration. The feasibility of the proposed galloping profile monitoring method has been demonstrated through laboratory experiments by considering three vibration patterns: vertical motion, horizontal motion, and nearly circular motion. The experimental results show that the proposed IMU reliably recognizes the vibration patterns, and satisfactorily reconstructs the galloping tracks of the power transmission line in all test cases.

5. ACKNOWLEDGEMENTS

The authors wish to acknowledge the financial support from the State Grid Henan Electric Power Research Institute (Grant No: 20131325).

REFERENCES

Den Hartog, J.P. (1932). "Transmission line vibration due to sleet." *Transactions of the American Institute of Electrical Engineers*, **51**(4), 1074-1076.

Desai, Y.M., Shah, A.H. and Popplewell, N. (1990). "Galloping analysis for two-degree-of-freedom oscillator." *Journal of Engineering Mechanics*, **116**(12), 2583-2602.

Desai, Y.M., Yu, P., Popplewell, N. and Shah, A.H. (1995). "Finite element modelling of transmission line galloping." *Computers & Structures*, **57**(3), 407-420.

Desai, Y.M. Yu, P., Shah, A.H. and Popplewell, N. (1996). "Perturbation-based finite element analyses of transmission line galloping." *Journal of Sound and Vibration*, **191**(4), 469-489.

Hu, Y. (2008). "Research on target detection and tracking algorithm based on monocular vision." *PhD Thesis*, Nanjing University of Science and Technology, Nanjing, China.

Huang, X., Huang, G. and Zhang, Y. (2009). "Designation of an on-line monitoring system of transmission line's galloping*." Proceeding of the 9th International Conference on Electronic Measurement & Instruments*, Beijing, China, 655-559.

Huang, X., Tao, B. and Feng, L. (2011). "Transmission lines galloping on-line monitoring system based on accelerometer sensors*." Proceeding of IEEE Power Engineering and Automation Conference*, Wuhan, China, 390-393.

Liu, C.S., Liu, H.Z., Jiang, D.Y., Jin, Y. and Zhang, L.H. (2014). "Research overview on galloping of iced transmission lines." *Science Technology and Engineering*, **14**(24), 156-164.

Liu, X.H., Yan, B., Zhang, H.Y. and Zhu, S. (2009). "Nonlinear numerical simulation method for galloping of iced conductor." *Applied Mathematics and Mechanics*, **30**(4), 489-501.

Madgwick, S.O.H., Harrison, A.J.L. and Vaidyanathan, R. (2011). "Estimation of IMU and MARG orientation using a gradient descent algorithm*." Proceeding of IEEE International Conference on Rehabilitation Robotics*, Zurich, Switzerland, 1-7.

Mitra, S.K. and Kuo, Y. (2006). *Digital Signal Processing: A Computer-based Approach*, Vol. 2, McGraw-Hill, New York.

Nigol, O. and Clarke, G.J. (1974). "Conductor galloping and control based on torsional mechanism*." Proceeding of IEEE Power Engineering Society Meeting*, New York, USA, Paper No. C74016-2.

Rui, X., Huang, H., Zhang, S. and Teng, W. 2011. "On-line monitoring system on power transmission line galloping based on fiber grating sensors*." Proceedings of the 30th Chinese Control Conference*, Yantai, China, 4327-4330.

Wang, Y.Y., Ren, H. and Du, L. (2010). "Analysis on conductor galloping track monitoring of transmission line." *Gaodianya Jishu/High Voltage Engineering,* **36**(5), 1113-1118.

Yu, P., Desai, Y.M., Popplewell, N. and Shah, A.H. (1993a). "Three-degree-of-freedom model for galloping. Part II: Solutions." *Journal of Engineering Mechanics*, ASCE, **119**(12), 2426-2448.

Yu, P., Desai, Y.M., Shah, A.H. and Popplewell, N. (1993b). "Three-degree-of-freedom model for galloping. Part I: formulation." *Journal of Engineering Mechanics*, ASCE, **119**(12), 2404-2425.